Journal of Applied Polymer Science

Effects of EPDM-g-MAH compatibilizer and internal mixer processing parameters on the properties of NR/EPDM blends: An analysis using response surface methodology

Jeefferie Abd Razak,[1,2] Sahrim Haji Ahmad,[1] Chantara Thevy Ratnam,[3] Mazlin Aida Mahamood,[2] Juliana Yaakub,[2] Noraiham Mohamad[2]

[1]School of Applied Physics, Faculty of Science and Technology, Universiti Kebangsaan Malaysia, 43600, UKM Bangi, Selangor, Malaysia

[2]Engineering Materials Department, Carbon Research Technology Research Group, Faculty of Manufacturing Engineering, Universiti Teknikal Malaysia Melaka, Hang Tuah Jaya, 76100, Durian Tunggal, Melaka, Malaysia

[3]Composites and Polymer Blends Group, Radiation Processing Technology Division, Malaysian Nuclear Agency, Bangi, 43000 Kajang, Malaysia

Correspondence to: J. A. Razak (E-mail: jeefferie@utem.edu.my)

ABSTRACT: This study evaluates the effects of ethylene-propylene-diene-monomer grafted maleic anhydride (EPDM-*g*-MAH) and internal mixer melt compounding processing parameters on the properties of natural rubber/ethylene-propylene-diene rubber (NR/EPDM) blends. Using Response Surface Methodology (RSM) of 2^5 two-level fractional factorial, we studied the effects of NR/EPDM ratio, mixing temperature, Banbury rotor speed, mixing period, and EPDM-*g*-MAH contents in NR/EPDM blends. The study found that the presence of EPDM-*g*-MAH in NR/EPDM blends had a predominant role as a compatibilizing agent, which affected the processability and properties of the final material. We also determined the model fitting with constant determination, R^2 of 99.60% for tensile strength (TS) response with a suggested combination of mixing process input parameters. The reproducibility of the proposed mixing strategy was then confirmed through model validation with a minor deviation at +2.303% and higher desirability of 0.960. This study is essential in providing a process design reference for NR/EPDM blends preparation by melt-blending and the role of a compatibilizer from the systematic Design of Experiment (DOE) approach. The experimental findings were further supported with swelling and cross-link density measurements, differential scanning calorimetry analysis, and observation of fracture morphology using a scanning electron microscope. © 2015 Wiley Periodicals, Inc. J. Appl. Polym. Sci. **2015**, *132*, 42199.

KEYWORDS: compatibilization; crosslinking; elastomers; rubber

Received 11 December 2014; accepted 13 March 2015
DOI: 10.1002/app.42199

INTRODUCTION

Numerous researches have reported on the preparation and characterization for various types of rubber blends.[1–4] The blending of rubber produces new materials with a wide range of applications by taking advantage from the attractive properties of the blend constituents, while avoiding the economic and technical uncertainties associated with synthesizing new polymeric materials.[5–7] Furthermore, the diversity of attractive rubber blend systems that have been commonly investigated, such as NR/SBR,[8] SBR/NBR,[2] NBR/EVA,[3] NBR/HNBR,[4] NR/BR/EPDM,[9] NR/SBR/BR,[10] NBR/EPDM,[11,12] NR/BR,[13] and many more, have sufficiently demonstrated the overwhelming need to identify versatile blends capable of meeting specific performances for certain technological usages. Among these, the vulcanized NR/EPDM systems have been extensively studied due to their superior performances in tires and other demanding applications.[6,14–22] Significant improvements in heat and ozone resistance[17] of NR/EPDM blends have attracted researchers to further explore and improvise the NR/EPDM compounds formulation.

EPDM is a saturated carbon-hydrogen polyolefinic rubber,[12] obtained by polymerizing ethylene and propylene with a small amount of a nonconjugated diene.[5,16] EPDM is often used as an impact modifier,[23] and the addition of this rubber phase in elastomer or thermoplastic elastomeric blends (TPE) imparts good ageing characteristics including weathering and oxidation, and thermal and chemical resistances.[16,22] However, the presence of EPDM in the formulation of rubber blends creates

major incompatibility and immiscibility problems due to the nonpolar and unsaturated characteristic of this synthetic rubber phase.[24]

In contrast with EPDM, NR is highly unsaturated and is chemically reactive.[19] Despite encompassing excellent elasticity, fatigue resistance, high resilience, and superior strength properties, low level of strain sensitivity, as well as good processing characteristics,[5,25] NR is highly susceptible to degradation. On top of that, NR is sensitive to environmental factors, such as ozone, light, moisture, humidity, radiation, and heat, due to its double bonds reactivity in the main chain.[5,14,26,27] This renders the use of NR not solely viable for many high-performance industrial applications.[28] Thus, blending of NR rubber with the low unsaturated rubber phase like EPDM (highly saturated and non-reactive),[14] can compensate for the limitations of NR.

Conversely, a higher cross-linking rate of NR has caused a selective diffusion of curatives towards the NR phase in any of their corresponding blends.[16] The lower solubility of many curatives in the EPDM phase could further reduce the propensity towards the formation of crosslink in the EPDM phase.[20] This scenario contributes to the uneven distribution of cure in the blend and poor interfacial adhesion between the phases, which results in major incompatibility and immiscibility problems between NR and EPDM,[16,20] that encourage the deterioration of the resulted properties and inferior performance of the blends.[17] Therefore, the ability to make virtually any two or more polymers to interact chemically with each other is highly desirable in manufacturing a wide variety of stable rubber blends.[21]

Some of the efforts that have been taken to improve the compatibility of the EPDM based rubber blends are slight precuring of EPDM before blending, radiation technique,[22] modification of EPDM with reactive chemicals like MAH,[6] functionalization of EPDM using halogenated and carboxylated EPDM,[25] mercapto-modified copolymer,[29] utilization of different accelerators and compatibilizers that have greater solubility with EPDM phase,[19,21] addition of a third rubber like ENR to act as a compatibilizer,[28] compounding technique, and addition of inorganic nanoparticles as an absorption and a stabilization agent at the interface of the blends.[14,17] Among these methods, the grafting of rubber phase with various functional monomers has been used as an effective tool for producing modified rubber blend with superior properties.[20,30] MAH or citric acid (or its hydrate) is a typical example of chemicals with two different functionalities used to compatibilize rubber blends via reactive blending approaches.[31] The polar character of the anhydride causes an affinity for the surface of the filler and the maleated polymer that can serve as a compatibilizer, which improves the interactions between the matrix and the filler.[30,32] Furthermore, grafting EPDM with MAH yields an elastomer which is characterized by local polarity and chemical reactivity.[9] In addition, upon our review of related studies carried out by previous researchers on EPDM grafted with MAH,[23,24,33,34] we found that if the EPDM molecules were functionalized by maleic-anhydride or maleic acid, the mechanical properties of the vulcanized blends of the functionalized EPDM with NR greatly improved.[9] This is because, the MAH group provides extra polarity to the EPDM and links to a high polar double bond of NR diene rubber phase.[9] MAH modification also increases the cross-link density in the EPDM phase, possibly because greater polarity leads to favorable distribution of curatives.[35] Moreover, EPDM-*g*-MAH has shown to be an efficient compatibilizer, with less processing difficulties than the commonly used ENR50 in NR filled nanoclay nanocomposites, as studied by Tavakoli *et al.*[36] Based on this observation, EPDM-*g*-MAH was chosen as a reactive compatibilizer agent to improve the interaction between NR and EPDM, as the compatibility between the two rubbers is the main factor that determines the properties of the blends.

Previous studies on NR/EPDM rubber blends have revealed that they can be prepared through various methods of compounding and mixing like a laboratory roll mill,[7,14,17,21,26] internal mixer,[5,16,19] and solvent removal from mixed polymer solution.[22] Of these processing techniques, melt blending provides extra benefits of simplicity, industrial scale-up, clean, less cost, is solvent-free and environmental friendly. In addition, it results in good end properties and the possibility to mass produce high performance polymer nanocomposites.[37] Thus, melt blending using an internal mixer was applied in this study. However, in dealing with an internal mixer, the properties of rubber blends are usually affected by the processing conditions and the composition of the blend, which require further optimization.[4,38] Previous researches,[6,14,25,39–41] only highlighted the effects like mixing speed, mixing period, and temperature in a one-factor-at-all time approach without considering the intercorrelation between the processing parameters to their output properties. Recently, Mohamad *et al.*[28,42] provided another alternative in rubber research for the optimization of melt-blending process parameters by integrating the statistical method of RSM in their experimental works and analysis. RSM provides a multifactor screening experiment without the issue of time constraint, but with higher reliability and capability in detecting the important process or system variables. It also eliminates the need for a large number of independent experiments, which are otherwise required in a conventional one-factor-at-a-time in the trial-and-error approach.[28,42,43]

In the present study, using RSM we studied the role of EPDM-*g*-MAH compatibilizer, coupled with the contribution of all processing parameters that were directly involved in melt blending operation using an internal mixer. Related literature on the development of rubber blends and the characterization of properties that integrate the statistical approaches are limited. Thus, this study reports the findings obtained from the polynomial mathematical model to represent the relationships between the content of EPDM-*g*-MAH compatibilizer, NR/EPDM blend ratio, and other internal mixer blending parameters (temperature, rotor speed, and mixing period) with respect to the resulted characteristics of cure and properties of mechanical tensile strength. Additionally, an analysis on the effect list and the interactions between the independent variables was also included. The findings were further supported by swelling and cross-link density measurements, glass transition temperature determination using DSC, and fracture surface morphological observation by SEM. The selection of the best combination of

Table I. Typical Compounding Formulation for NR/EPDM Blends Preparation

Ingredient	Loading (phr)[a]
Rubber blend[b]	100.00
Zinc oxide	5.00
Stearic acid	2.00
6-PPD[c]	2.00
CBS[d]	1.00
TMTD[e]	0.30
Sulfur	1.50
EPDM-*g*-MAH[f]	1.00–5.00

[a] Parts per hundred rubber.
[b] NR/EPDM at 70 : 30, 60 : 40 or 50 : 50 ratio.
[c] *n*-(1,3-Dimethylbutyl)-*n*′-phenyl-*p*-phenylenediamine.
[d] *n*-Cyclohexylbenthiazyl sulfenimide.
[e] Tetramethylthiuram disulfide.
[f] Ethylene propylene diene monomer grafted maleic anhydride.

processing parameters was then conducted using an optimization menu in Design Expert 6.0.10 software, which provided a process design reference on systematic preparation of NR/EPDM blends with improved end properties.

EXPERIMENTAL

Raw Materials

The formulation used in the present study is shown in Table I. NR with commercial trade name of SMR20 grade was supplied by Malaysian Rubber Board (LGM) with 0.16 max. % wt dirt retained on 44 apertures, 1.00 max. % wt ash content, 0.60 max. % wt nitrogen, 0.80 max. % wt volatile matter, 30 min Wallace rapid plasticity (P_o), and 40 min % of plasticity retention index (PFU). Ethylene propylene diene rubber (EPDM) grade BUNA® EPT 9650 procured from LANXESS, Pittsburgh, with Mooney viscosity UML (1 + 8) at 150°C is 60 ± 6 MU, ethylene content 53 ± 4 wt %, ENB content 6.5 ± 1.1 wt % with volatile matter ≤0.75 wt %, specific gravity 0.86, and total ash ≤0.50 wt % with non-staining stabilizer was used. Both rubbers were masticated with two-roll mill for about 10 min at 30°C, prior of their use. Other compounding ingredients, such as sulfur, zinc oxide, and stearic acid, were purchased from Systerm/Classic Chemical Sdn. Bhd., and tetramethylthiuram disulfide (Perkacit-TMTD) from Aldrich Chemistry; and *n*-cyclohexylbenthiazyl sulfenimide (CBS), and *n*-(1,3-dimethylbutyl)-*n*'-phenyl-*p*-phenylenediamine (6PPD) were supplied by Flexys America. All compounding chemicals were used as received without further steps of purification. The MAH used was a synthesis grade (95% that may contain ≤5% of maleic acid), while the DCP used was *bis*(1-methyl-1-phenylethyl) peroxide, *bis*(α,α-dimethylbenzyl peroxide) with molecular formula weight of 270.37, vapor density of 9.30, and vapor pressure of 15.40 mmHg, and both were supplied by Sigma Aldrich, Germany.

Preparation and Characterization of EPDM-*g*-MAH Compatibilizer

The EPDM-*g*-MAH compatibilizer was synthesized on a lab scale via a melt-compounding method using Haake Polylab OS RheoDrive 16 internal mixer with Banbury rotor and 0.70 of filling factor. An FTIR evaluation for MAH was obtained through a standard KBr method. EPDM was first masticated at 30°C for 10 min by using a two-roll mill, and was followed by a melt-blending with peroxide initiated grafting strategy at 180°C, 75 rpm of rotor speed, and 5 min of grafting. The grafted compound was conditioned at 25°C for 24 h and hot compression molded at 150°C for 10 min, and 5 MPa of compression pressure for thin film preparation at 200 to 250 μm thickness. The films were conditioned in an air drying oven at 75°C for 10 h to eliminate the unreacted MAH. The validation of grafting was done by using the attenuated total reflectance of ATR-FTIR model Jasco Pro 450-S spectrometer from 4500 to 400 cm^{-1} wavenumber with 4.0 cm^{-1} resolution and 50 scans.

Design of Experiment

An experimental design was performed using Design Expert software (Statistics Made Easy, version 6.0.10, Stat-Ease, Minneapolis, MN). A two-level fractional factorial design of the experiment was utilized in this study with independent variables involved, namely NR/EPDM ratio (X_1), mixing temperature (X_2), rotor speed (X_3), mixing period (X_4), and EPDM-*g*-MAH content (X_5). A 2^5 fractional factorial design for five independent variables with three replications at center point and no blocks were implemented to yield 19 sets of experiments. The levels of independent variables are summarized in Table II. The factorial designs of the experiments for all the parametric combinations are listed in Table III. This study reported four dependent variables that consisted of maximum curing time, tc_{90} (Y_1), and maximum torque, M_H (Y_2), which represent the characteristic of cure for blend processability, while tensile strength, TS (Y_3), and the percentage of elongation at break, EB (Y_4), *in lieu* of the evaluation of mechanical properties. Furthermore, the RSM method was applied in the polymer research to determine the quantitative equations with a minimal number of experiments, as previously reported by Mohamad *et al.*[28,42] In this present study, the effects of the addition of compatibilizer and its correlation with processing parameters on the resulted properties of NR/EPDM blends were evaluated through the statistical approaches.

Melt Compounding, Characteristic of Cure, and Preparation of Sample

The process of melt compounding for NR/EPDM blends was performed using Haake Polylab OS RheoDrive 16 internal mixer with Banbury rotor in accordance to ASTM D3192 for semi-EV sulfur vulcanization system.[28] The recipes for the compounding formulation can be referred to a Table I, and the blending operation was performed following the combination of parameters generated by the Design Expert software 6.0.10 based on a fractional two-level factorial design, as tabulated in Table III. Both NR and EPDM rubber were first masticated at 30°C for 10 min by using two-roll mill to reduce the molecular weight of rubber to ease the subsequent melt-blending steps. As for compounding with an internal mixer, the NR, EPDM and EPDM-*g*-MAH were firstly added. Then a first set of curatives, which consisted of zinc oxide, stearic acid and CBS, was added after 2 min of compounding period. Finally, a second set of curatives that consisted of sulfur and accelerator like 6PPD and TMTD was added a minute before the mixing ended. The compounds were

Table II. Levels of Each Independent Variable

NR/EPDM ratio (X_1: phr)	Mixing temperature (X_2: °C)	Rotor speed (X_3: rpm)	Mixing time (X_4: min)	EPDM-*g*-MAH content (X_5: phr)
70 : 30 (−1)	70 (−1)	50 (−1)	5 (−1)	1 (−1)
60 : 40 (0)	90 (0)	60 (0)	7 (0)	3 (0)
50 : 50 (+1)	110 (+1)	70 (+1)	9 (+1)	5 (1)

dumped and left to cool at room temperature for 24 h before cure characteristic assessment.

The processability of NR/EPDM blends were then tested with cure characteristic assessment in accordance with ASTM D 2084 using an oscillating rotorless rheometer U-CAN Dynatex UR2010 (U-Can Incorporation, Taiwan). The samples of the respective blends were tested at 160°C, 4.5 kg/cm^2 of compression pressure, 1.7 Hz of swing frequency, and +1° swing amplitude within 5 min of curing time. The maximum curing time, tc_{90} and the maximum torque (M_H) were determined in this assessment. The compounds of the rubber blend were subsequently molded with compression machine at 160°C and 150 kgf using a hot press model GT7014-A, GoTech (Korea), based on the respective maximum cure time, tc_{90} was obtained from the cure characteristic testing. The molded compounds were conditioned before testing and further analysis.

Mechanical Tensile Testing

A tensile testing of NR/EPDM rubber blends was carried out in accordance to ASTM D 1822 on a Universal Testing Machine model Toyoseiki Strograph-R1 (Japan). Before that, dumb-bell shaped specimens were cut from the molded sheet using a SDL-100 (Japan) SD-type lever controlled sample cutter. The samples were tested at a crosshead speed of 500 mm/min and the test was performed at 23 ± 2°C. At least seven samples from each compound were tested to ensure a high confidence level in the experimental results. The tensile properties such as tensile strength (TS) and the percentage of elongation at break (EB) were determined in this testing. The following equation was used for the calculation of EB value.[44]

$$\text{EB} = \frac{\text{Displacement at failure}}{\text{Effective gauge length}} \times 100 \quad (1)$$

Swelling and Cross-Linking Density Measurements

Swelling tests were performed using cured samples in accordance with ISO 1817. The specimens (dimension: 20 mm length × 20 mm width × 2mm thickness) were weighed using an electronic top loading balance AB135-S/FACT Mettler Toledo, followed by immersion in toluene until equilibrium was achieved for 72 h at room temperature (25°C) in a dark environment.[7]

Table III. Parametric Combination by 2^5 Fractional Two-Level Factorial Design Matrix

		Coded variable				
Experiments	Sample code	NR/EPDM ratio (X_1)	Mixing temperature (X_2)	Rotor speed (X_3)	Mixing time (X_4)	EPDM-*g*-MAH content (X_5)
1	R1	−1	−1	−1	−1	+1
2	R2	+1	−1	−1	−1	−1
3	R3	−1	+1	−1	−1	−1
4	R4	+1	+1	−1	−1	+1
5	R5	−1	−1	+1	−1	−1
6	R6	+1	−1	+1	−1	+1
7	R7	−1	+1	+1	−1	+1
8	R8	+1	+1	+1	−1	−1
9	R9	−1	−1	−1	+1	−1
10	R10	+1	−1	−1	+1	+1
11	R11	−1	+1	−1	+1	+1
12	R12	+1	+1	−1	+1	−1
13	R13	−1	−1	+1	+1	+1
14	R14	+1	−1	+1	+1	−1
15	R15	−1	+1	+1	+1	−1
16	R16	+1	+1	+1	+1	+1
17	R17	0	0	0	0	0
18	R18	0	0	0	0	0
19	R19	0	0	0	0	0

The swollen samples were removed after the immersion period and were weighed. The specimens were then dried in an oven at 60°C until a constant weight was obtained. The change in mass was referred to as the percentage of swelling and is given as in eq. (2):[24]

$$\text{Swelling } (\%) = \frac{(W_2 - W_1)}{W_1} \times 100 \quad (2)$$

where W_1 is the initial mass (g), and W_2 is the mass (g) after immersion in toluene. By applying the Flory-Rehner equation, the molecular weight between the crosslink (M_c) and the crosslink density (V_c) or the concentration of elastically effective chains were calculated based on the swelling test results. This parameter included the true chemical crosslink and the physical crosslink, such as chain entanglements and loops.[7] The Flory-Rehner equations are illustrated in the following eqs. (3)–(5):

$$M_c = \frac{-\rho_p V_s V_r^{1/3}}{\ln(1-V_r) + V_r + \chi V_r^2} \quad (3)$$

$$V_r = \frac{1}{1 + Q_m} \quad (4)$$

$$V_c = \frac{1}{2M_c} \quad (5)$$

where ρ is the rubber density ($\rho_{NR} = 0.92$ g/cm^3; $\rho_{EPDM} = 1.06$ g/cm^3), V_s is the molar volume of toluene ($V_s = 106.4$ cm^3/mol), V_r is the volume fraction of the polymer in the swollen specimen, Q_m is the increased weight of the blends in toluene, and χ is the interaction parameter of the rubber network-solvent (χ of NR = 0.393; χ of EPDM = 0.49).

Thermal Analysis by Differential Scanning Calorimeter

Heat flow analysis was performed by using a Differential Scanning Calorimeter, DSC-1 Jade by Perkin Elmer. It was performed between −65 and 150°C, with 20°C/min of heating rate, and nitrogen gas was purged at a flow rate of 20 mL/min. About ~5 to 10 mg of the sample was weighed and was placed in a crimped standard aluminum pan. The first scanning of heating endotherms were analyzed and the glass transition temperature (T_g) was determined from the primary point that intersected the tangent discontinuity in the DSC curve.[11]

Observation of Fracture Morphological Using Scanning Electron Microscopy

The selected tensile fractured specimens were placed on an aluminum stub with carbon tape. Later, the specimens were sputter coated with a thin layer of gold using Polaron E-1500 to avoid electrostatic charge and poor images during observation. The morphologies of NR/EPDM blends were observed at 300× and 5000× magnification with a variable pressure scanning electron microscope (VPSEM) model Zeiss Evo-50 operated at 15 kV of the accelerating voltage with secondary electron (SE) mode signal detector.

RESULTS AND DISCUSSION

Characterization for EPDM-*g*-MAH Compatibilizer

Figure 1 provides the comparisons of FTIR spectra between pure EPDM, MAH, and EPDM-*g*-MAH. The analysis on pure EPDM rubber spectra showed the presence of bands at 1466 and 1376 cm^{-1} that were assigned to —CH_2 scissoring vibration and C—H bending vibration of —CH_3 from the propylene unit, respectively. The band at 711 cm^{-1} was typical of $(CH_2)^n$, where $n \geq 5$ for CH_2 rocking vibration due to the presence of ethylene in the EPDM backbone. In addition, the peaks at 2926 and 2856 cm^{-1} were typical of EPDM rubber arising from the saturated hydrocarbon backbone of aliphatic alkyl symmetric or asymmetric C—H stretching vibration.[16] IR spectra for EPDM-*g*-MAH were referred. The absorption bands at the region of 1770 to 1792 cm^{-1}, which attributed to C═O symmetric stretching bonds, were related to successful MAH grafted to the EPDM rubber.[23] The peak at 1713 cm^{-1} was attributed to the presence of dimeric carboxylic acid in the EPDM-*g*-MAH sample. In addition, the existence of OH group in EPDM-*g*-MAH was confirmed with the presence of absorption peak at 922 cm^{-1}.[23,24] The missing absorption peak at 1779 to 1780 cm^{-1} (C—O stretching for anhydrides) for the pure EPDM sample confirmed the success of EPDM grafting reaction with MAH.

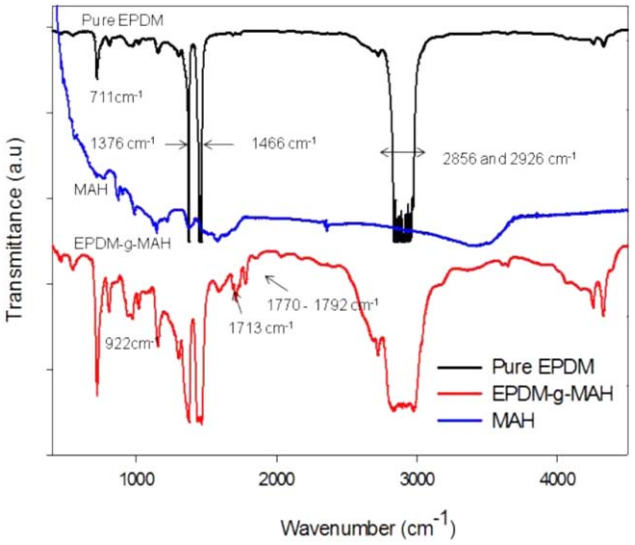

Figure 1. FT-IR spectra for pure EPDM, MAH and EPDM-*g*-MAH. [Color figure can be viewed in the online issue, which is available at wileyonlinelibrary.com.]

Regression Equation for Selected Models

The polynomial relationships for the responses studied were derived from our experimental findings. The application of experimental design to fit the results with a first-order polynomial equation, which included all interaction terms, referred to the principles explained in the previous works reported by other co-workers.[28,42] The variation introduced in this present study was compared with those presented by Mohamad *et al.*,[28] whereby five independent variables ($k = 5$) were applied instead of four, EPDM-*g*-MAH was used as the compatibilizer and not the ENR-50 as the third rubber phase, and there were differences in the range for certain variables. In addition, the regression equations for responses in this study were obtained using the RSM statistical approach that consisted of Y_1: maximum curing time (tc_{90}), Y_2: maximum torque (M_H), Y_3: tensile strength (TS), and Y_4: percentage of elongation at break (EB). The five

Table IV. Regression Models of Each Response

Responses	R^2	Adjusted R^2	Polynomial relationships
$Y_1 = tc_{90}$	0.9976	0.9862	$Y_1 = +3.19 + 0.32X_1 - 0.27X_2 - 0.092X_3 - 0.052X_4 + 0.11X_5 + 0.098X_1X_2 + 0.020X_1X_4 + 0.10X_1X_5 - 0.084X_2X_3 - 0.061X_2X_4 - 0.043X_2X_5 + 0.077X_3X_4 + 0.012X_3X_5 - 0.033X_4X_5$
$Y_2 = M_H$	0.9992	0.9930	$Y_2 = +23.41 - 0.52X_1 + 0.72X_2 + 0.15X_3 - 0.28X_4 - 0.038X_5 - 0.41X_1X_2 - 0.37X_1X_3 - 0.21X_1X_4 - 0.13X_1X_5 + 0.29X_2X_3 + 0.44X_2X_4 - 0.17X_2X_5 - 0.38X_3X_4 - 0.037X_3X_5 - 0.11X_4X_5$
$Y_3 = TS$	0.9960	0.9865	$Y_3 = +5.39 - 0.095X_1 - 0.29X_2 - 0.016X_3 - 0.42X_4 - 0.16X_5 - 0.26X_1X_3 + 0.085X_1X_4 - 0.13X_1X_5 - 0.25X_2X_3 + 0.24X_2X_5 - 0.10X_3X_4 + 0.13X_4X_5$
$Y_4 = EB$	1.0000	0.9997	$Y_4 = +638.99 - 4.84X_1 - 114.69X_2 + 51.31X_3 - 30.13X_4 + 28.01X_5 + 3.24X_1X_2 + 7.43X_1X_3 + 54.38X_1X_4 + 12.99X_1X_5 - 6.28X_2X_3 - 2.91X_2X_4 - 6.69X_2X_5 + 53.48X_3X_4 - 10.76X_3X_5 + 51.75X_4X_5$

independent variables involved were: X_1: NR/EPDM ratio, X_2: mixing temperature, X_3: rotor speed, X_4: mixing time, and X_5: EPDM-*g*-MAH compatibilizer content. Besides that, the selected model by RSM for each response was based on the highest priority in accordance with the polynomial level and the lowest P value.[28] Thus, the mathematical relationship connecting the variables and the predicted responses is presented as eq. (6):

$$Y = B_o + B_1X_1 + B_2X_2 + B_3X_3 + B_4X_4 + B_5X_5 + B_{12}X_1X_2 + B_{13}X_1X_3 + B_{14}X_1X_4 + B_{15}X_1X_5 + B_{23}X_2X_3 + B_{24}X_2X_4 + B_{25}X_2X_5 + B_{34}X_3X_4 + B_{35}X_3X_5 + B_{45}X_4X_5 \quad (6)$$

where Y is the predicted response; B_o is the offset term; B_1, B_2, B_3, B_4, and B_5 are the linear coefficients; B_{12}, B_{13}, B_{14}, B_{15}, B_{23}, B_{24}, B_{25}, B_{34}, B_{35}, and B_{45} are the cross-product coefficient; and X_1, X_2, X_3, X_4, and X_5 are the independent variables. The regression model for each response, their coefficient of determination values R^2, and adjusted R^2 are presented in Table IV. All the terms included in each equation represented the mathematical relationship between the quantitative effects of the independent variables and their interaction to the response.

The intercept for each response was the grand average of all 19 observations, while the regression coefficient was one-half of the corresponding factor effect estimated based on two-unit change. Positive coefficient values reflect the increasing effects on the response, while the negative values provide opposite effects. The R^2 values indicate the degree of agreement between the experimental results and those predicted by the regression model. The R^2 values for all responses were obtained in the range of 0.90 to 0.99, which were very close to union ($R^2 = 1.00$), almost 100% of the variation in the overall system was presented by the model. This indicates that the regression model was accurate in describing and predicting the pattern of significance for each factor studied and could be used to navigate the design space.[28] The list of effects for each contributed term to the response studied is listed in Table V.

On top of that, the response of tensile strength (TS) was taken as an example for the explanation of the list of effects (Table V). It demonstrated that the mixing period (X_4) was listed as the most significant factor with a greater percentage of contribution (26.20%), whereas the rotor speed (X_3) contributed less to the response with only 0.038% of contribution. Here, the mixing period was controlled, as a longer exposure of the blended macromolecular chains would lead to degradation due to excessive heat and shearing action by rotor blade, while shorter period of exposure would refrain from stabilization in processing torque that would lead to incompatibility and separation between phases.

Furthermore, small values for some terms of interaction in the list of effects, such as X_1X_2, X_2X_4, and X_3X_5, indicated the insignificant contribution to the response and the interaction between them was negligible and was not even considered in the regression equation of Y_3 for TS. The polynomial relationship for Y_3 is depicted in Table IV. Here, the negative value for each single variable in Y_3 suggested that the decreasing coefficient value for X_1, X_2, X_3, X_4, and X_5 from the higher level to the lower level increased the value of output response.

Table V. The Effect List of Each Terms Contributing to the Response

Percentage of contribution to each response (%)				
Term	tc_{90}	M_H	TS	EB
X_1	39.01	15.06	1.32	0.089
X_2	27.79	28.64	12.21	49.73
X_3	3.21	1.28	0.038	9.95
X_4	1.04	4.22	26.20	3.43
X_5	4.31	0.081	3.61	2.97
X_1X_2	3.65	9.58	2.399E-003	0.040
X_1X_3	0.011	7.56	9.95	0.21
X_1X_4	0.15	2.51	1.06	11.18
X_1X_5	4.05	0.94	2.61	0.64
X_2X_3	2.72	4.57	8.80	0.15
X_2X_4	1.44	10.87	1.420E-005	0.032
X_2X_5	0.69	1.70	8.47	0.17
X_3X_4	2.27	7.95	1.54	10.81
X_3X_5	0.060	0.076	7.510E-003	0.44
X_4X_5	0.42	0.67	2.31	10.13
Curvature	8.97	4.22	21.57	0.031

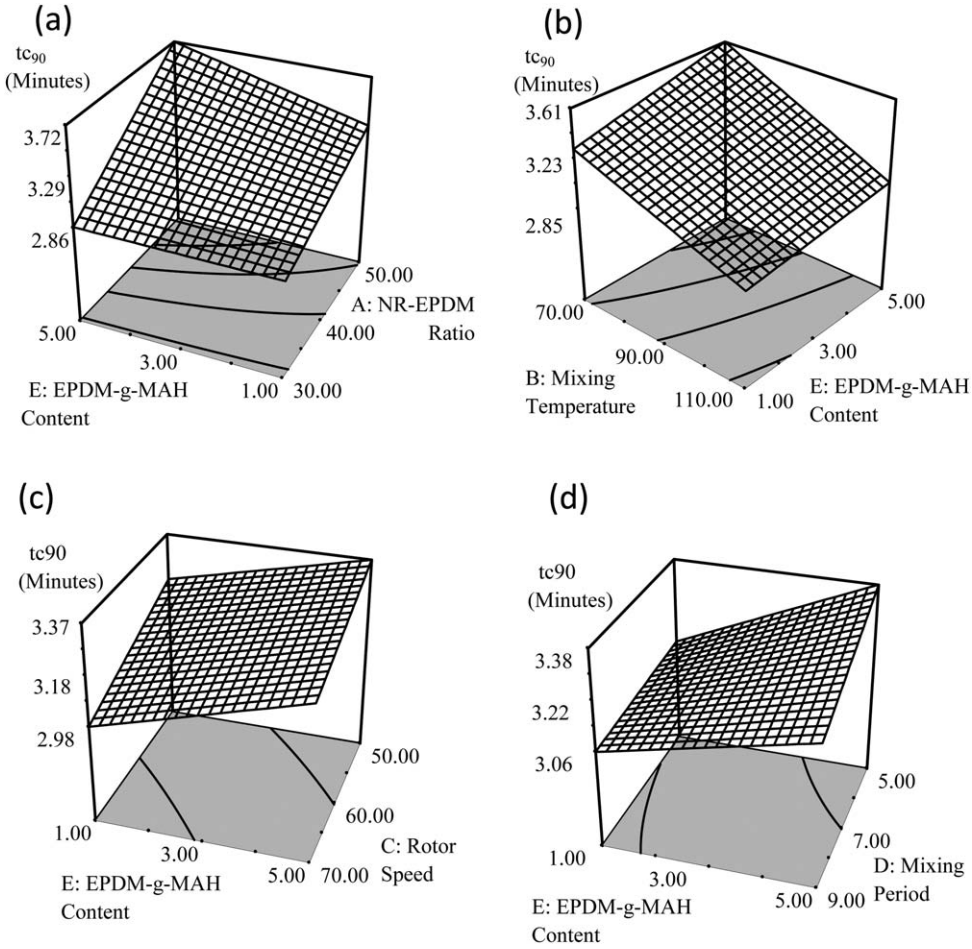

Figure 2. Response surface plots showing variation in interaction between variables for tc_{90}: (a) X_1X_5; (b) X_2X_5; (c) X_3X_5, and (d) X_4X_5.

Meanwhile, the positive coefficient value for several terms of interaction in Y_3 response indicated good dependency between the corresponding variables in affecting the TS of NR/EPDM blends. On the other hand, as for Y_1, Y_2, and Y_4 responses, all the individual and terms of interaction were primarily considered in the regression equation, indicating the considerable contribution for each independent variable to the response with the list of effects that evidenced their role quantitatively (Table V).

Interaction Between Variables on Response Surface Plots

Maximum Cure Time, tc_{90} (Y_1). Maximum cure time is the time required to reach 90% of full cure and is generally the state of cross-linking at which the most physical properties of the rubber blend reach optimal results. It is crucial to control this attribute to avoid the reverse curing phenomena due to compound over cure, where the blend becomes soft and less elastic, but more plastic.[2] From the response plots [Figure 2(a)], the increase in maximum cure time was proportional with the increase of the EPDM content up to 50 phr of EPDM in NR/EPDM ratio and the content of EPDM-*g*-MAH compatibilizer up to 5 phr. This can be attributed to the lower efficiency of the EPDM rubber to be vulcanized with the sulfur system. EPDM has a comparatively low diene content and lower unsaturation chain level as compared than NR.[6] This, was further supported by El-Sabbagh,[34] in their study on NR/EPDM blend. They found that the higher EPDM ratio in the blend increased the characteristic of curing. Furthermore, Botros and El Sayed,[6] also found that the addition of compatibilizer into the NR/EPDM blend increased the M_H and tc_{90}. Similar to the tc_{90} response, the scorch time (ts_2) was directly proportional with the increase of EPDM and EPDM-*g*-MAH compatibilizer in the blends. Generally, the ts_2 can be correlated to the time required for the state of cure to increase up to two torque units above the minimum at a given cure temperature.

From the interaction between the mixing temperatures versus EPDM-*g*-MAH content, it was found that lower mixing temperature and maximum amount of EPDM-*g*-MAH yielded a higher tc_{90} value [Figure 2(b)]. Furthermore, there were almost insignificant effects between the rotor speeds and the added compatibilizer, as portrayed in Figure 2(c), due to a less gradient plot for both variables (X_3X_5). In addition, a lower percentage of contribution in the list of effects for these terms of interaction (Table V) might have supported this situation. Rotor speed did not change the response to be either at lower (50 rpm) or at higher speeds (70 rpm) with the increased content of the EPDM-*g*-MAH compatibilizer [Figure 2(c)]. The interaction between the mixing periods and the EPDM-*g*-MAH, as

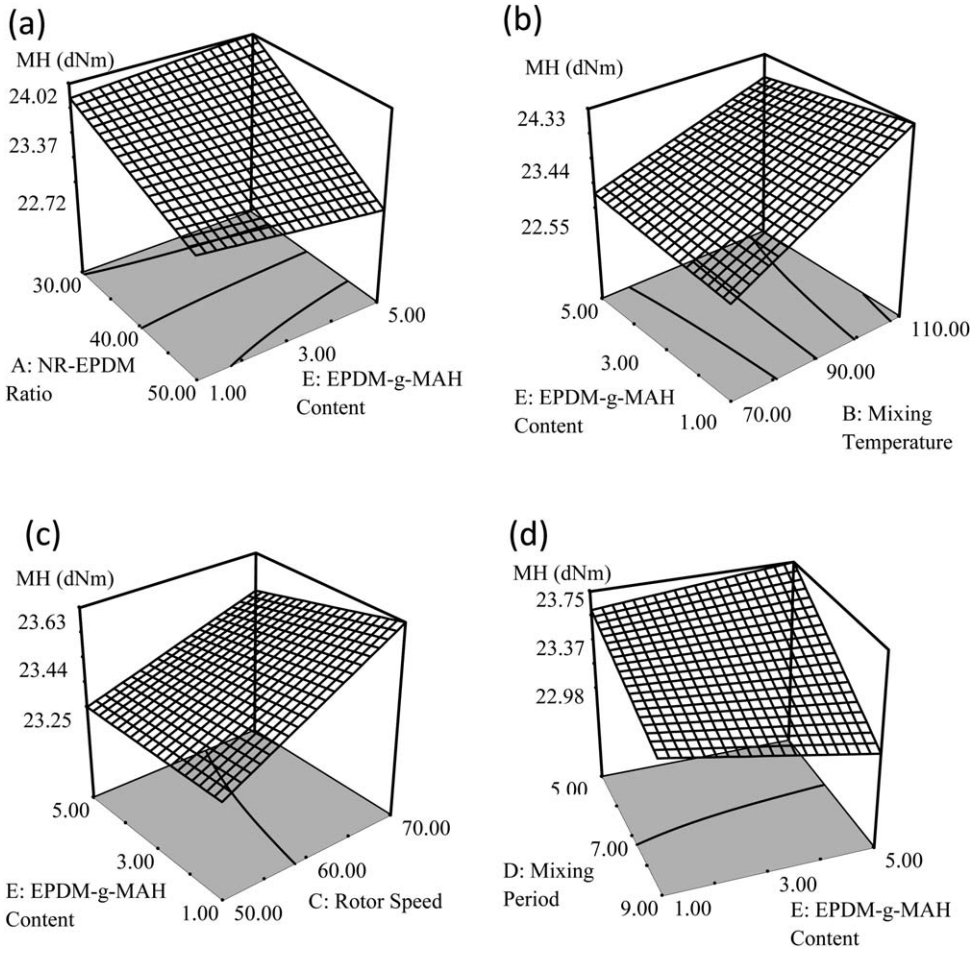

Figure 3. Response surface plots showing variation in interaction between variables for M_H: (a) X_1X_5; (b) X_2X_5; (c) X_3X_5, and (d) X_4X_5.

illustrated in Figure 2(d), predetermined that higher tc_{90} could be obtained by using the maximum amount of the EPDM-*g*-MAH compatibilizer at a shorter period of compounding.

In relation to the measurement of the vulcanization rate based on the differences between the optimum vulcanization (tc_{90}) and the scorch time (ts_2) which yielded the cure rate index (CRI), the decrease in the CRI indicates a decrease in the number of reactive sites for cross-linking reaction in the blends. Thus, the variation in CRI due to the presence of the EPDM-*g*-MAH compatibilizer showed the role of MAH in affecting the crosslink distribution which led to the bonding or compatibility between NR and EPDM rubber phases.

Maximum Torque, M_H (Y_2). M_H indicates the maximum torque achieved during the curing or the degree of cross linking.[25] The higher the torque obtained, the higher the number of crosslink created.[45] M_H also represents the vulcanizates strength of rubber blend compounds.[46] Figure 3(a) demonstrates the maximum torque versus EPDM-*g*-MAH and NR/EPDM ratio in a three-dimensional surface plot. The value of M_H increased with the decrease of NR/EPDM ratio (lower EPDM content), together with the factors of EPDM-*g*-MAH in the blends. The variation in M_H can be attributed to the higher plasticity and Mooney viscosity of the EPDM component in the NR/EPDM blends.[6] These findings are in line with Shehata's *et al.*, who found that the addition of compatibilizer into a 50/50 NR/EPDM blend increased M_H that gave rise to the enhancement of the cross linking that took place during the curing process. This can be considered a good sign for the compatibility between the NR and the EPDM rubber phase.[21] A comparable pattern for the torque difference of M_H-M_L as observed in this study provides a measure of shear dynamic modulus that directly supports the attainment of a characteristic network chains in the blends as indicated by similar trend to M_H.

A higher maximum torque also confirmed an adequate interaction in the phase of blend in terms of their molecular network. Hence, good interaction in the blends was attributed to reactive compatibilization between polar groups of EPDM-*g*-MAH and carbon-carbon double bond of the unsaturated rubber.[28] Besides that both rotor speed and mixing period showed insignificant interaction with the presence of EPDM-*g*-MAH as per agreed by the lowest percentage of contribution in the list of effects at 0.076 and 0.67 for X_3X_5 and X_4X_5, respectively (Table V).

Tensile Strength, TS (Y_3). The effects of the addition of the EPDM-*g*-MAH compatibilizer and their correlation with other

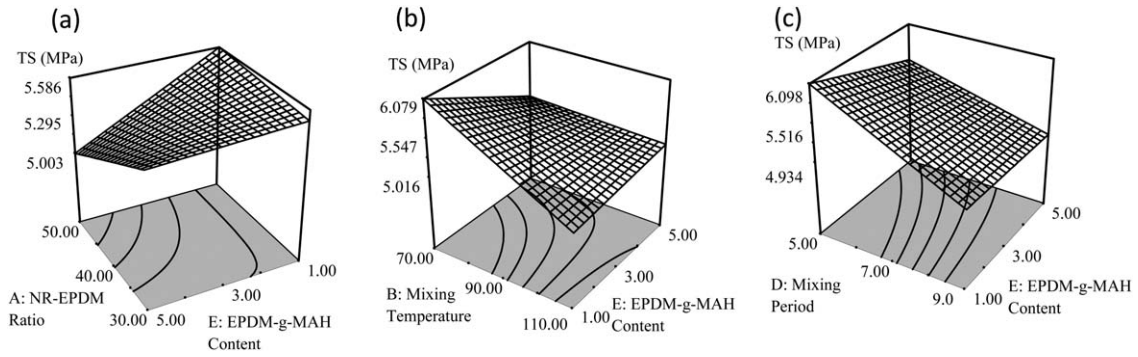

Figure 4. Response surface plots showing variation in interaction between variables for TS: (a) X_1X_5; (b) X_2X_5, and (c) X_4X_5.

melt-compounding processing parameters for TS of NR/EPDM blends are shown in Figure 4. No response plots for X_3X_5 term of interaction was available due to the lowest percentage of contribution towards Y_3 in the list of effects, indicating insignificant interaction between those variables. Figure 4(a) depicts the effects of NR/EPDM ratio versus EPDM-*g*-MAH content.

Tensile strength increased with the increase in the content of EPDM up to 50 phr in the NR/EPDM blend with the decreased content of the EPDM-*g*-MAH compatibilizer to 1 phr. In contrast, the TS for a 50/50 NR/EPDM blend with a higher EPDM-*g*-MAH content (5 phr) experienced significant reduction to a minimum TS value due to the domination of the EPDM rubber in the formulation of the blend. EPDM had lower strength than NR. Thus, a higher EPDM content in the compound resulted in a lower TS output. In this case, it is believed that a minimum amount of EPDM-*g*-MAH content was sufficient to provide the best compatibilization effects that induced in situ formation of compatibilizing interchain copolymer between the EPDM and NR rubbers.[28] The NR/EPDM blend with lower EPDM, but higher NR ratio (70 : 30) with only 1 phr of EPDM-*g*-MAH had considerably higher TS, indicating the efficacy of the added compatibilizer to provide a good interaction at the interface between the rubber phases. Moreover, the NR rich blend exhibited higher TS due to NR crystallinity exhibited upon stretching.[16] This situation was further supported by a comparable pattern of modulus at 100, 300, and 500% of elongation (M100, M300, and M500). The incorporation of EPDM-*g*-MAH compatibilizer to the NR/EPDM blends increased the rigidity of vulcanizates. The compatibilizer added at a minimal amount introduces an excellent interfacial adhesion between NR and EPDM rubber phases. This has directly hindered the chain sliding past one another when the samples are placed under tensile loading. The resistance to deformation is enhanced and thus resulting better stiffness of the NR/EPDM blends.

On the effect of mixing temperature versus the addition of EPDM-*g*-MAH compatibilizer [Figure 4(b)], it was found that at higher mixing temperatures with maximum content of EPDM-*g*-MAH added to the blend, the response of TS was reduced to minimum output. In this case, a lower amount of EPDM-*g*-MAH compatibilizer is in fact efficient in its function to enhance TS at a lower mixing temperature. Based on these findings, higher mixing temperatures are not recommended in the preparation of the NR/EPDM blend as it is prone to cause heat degradation that would later diminish the properties of the blend and hinder the function of the compatibilizer.

Figure 4(c) depicts the relationship between the mixing period and the EPDM-*g*-MAH content added to the NR/EPDM blend. A shorter mixing period (5 min) versus a lower amount of EPDM-*g*-MAH addition (1 phr) yielded higher TS. Moreover, a maximum mixing period was found to yield a minimum result for TS, while longer mixing period intensified the damage in the rubber chain and cross-linking due to the extended exposure to heat and strong shearing forces by Banbury rotor rotation. A shorter mixing period was more beneficial as it eliminated the longer mixing cycles, and was more economical for the blend processing.

Thus, overall, the response surface plot for the terms of interaction for X_1X_5, X_2X_5, and X_4X_5 showed that a little amount of EPDM-*g*-MAH was required to provide maximum effect of compatibilization in enhancing the interaction between NR and EPDM rubber phases. In addition, the presence of polar groups in EPDM-*g*-MAH enhanced the distribution of EPDM in the NR matrix, and thus, improved the properties of mechanical tensile strength.[28] SEM observations on the fractured samples are depicted in Figure 9 to further support the variation that occurred in the findings of TS.

Percentage of Elongation at Break, EB (Y_4). Figure 5(a) shows the correlation between NR/EPDM ratios and the content of EPDM-*g*-MAH compatibilizer in rubber blends. A maximum amount of EPDM-*g*-MAH at 5 phr was required to optimize the EB response for NR/EPDM blends with either lower (70 : 30) or higher (50 : 50) formulation of EPDM content blends. The EB increased in parallel with the increase of EPDM-*g*-MAH content. The added compatibilizer acted as anchor points between the molecular chains for both the rubber phases and extended the elongation towards a higher degree during the tensile loading by preventing chain slippage from occurring.[28] This, allowed the blend with higher EPDM-*g*-MAH content to be elongated in a higher percentage of elongation compared with neat NR/EPDM blend and possibly introduced the strain induces crystallization phenomena that further supported the improvement in TS, M100, M300, and M500.

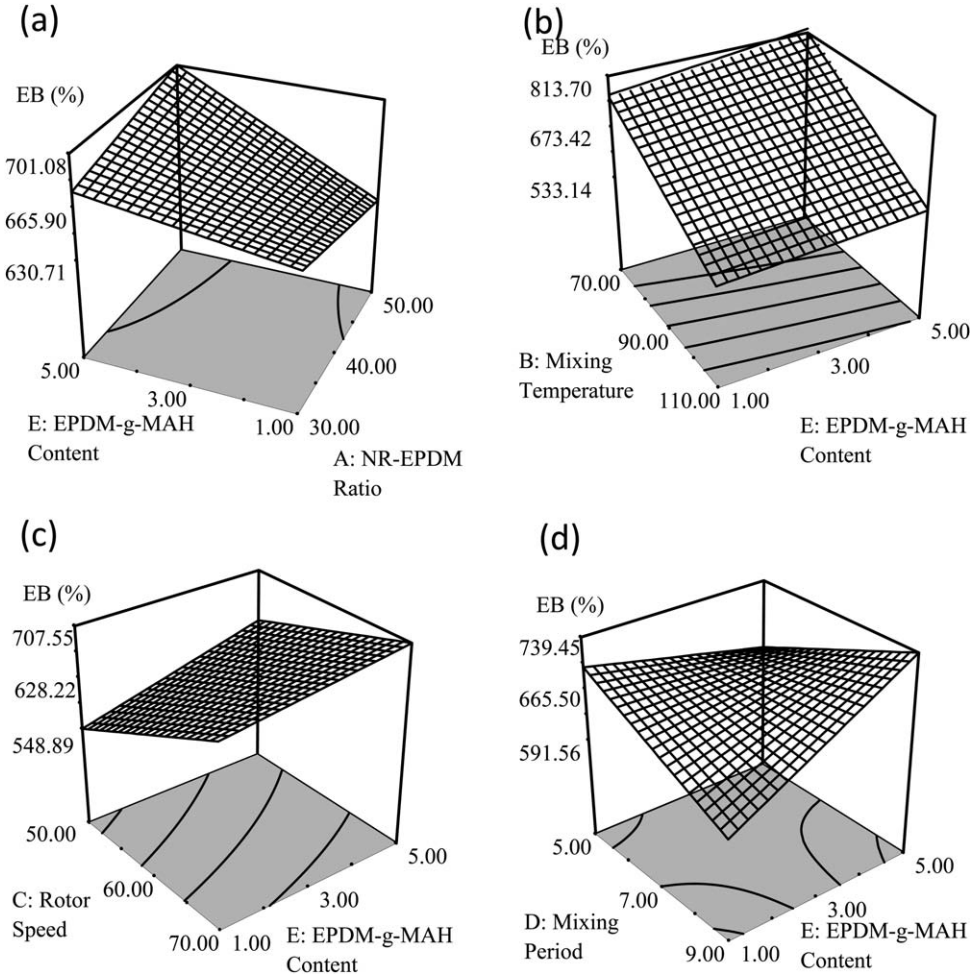

Figure 5. Response surface plots showing variation in interaction between variables for EB: (a) X_1X_5; (b) X_2X_5; (c) X_3X_5, and (d) X_4X_5.

The response surface plot for the interaction between the mixing periods and the EPDM-*g*-MAH content, X_4X_5, is depicted in Figure 5(d). There were two maximum conditions for EB: (a) when there was lower addition in the content of EPDM-*g*-MAH (1 phr for 5 min of mixing period), and (b) there was higher addition in the content of EPDM-*g*-MAH (5 phr at 9 min of mixing period). However, the lowest EB response for X_4X_5 interaction was obtained when a minimum EPDM-*g*-MAH compatibilizer was added for compounding with extended period up to a maximum of 9 min. These situations showed that a longer mixing period did not definitely assured the enhancement of EB response, whilst to some extent, only a small amount of EPDM-*g*-MAH compatibilizer was required to improve the compatibility between the rubber phases with regards to the mixing time parameter.

The interaction for EPDM-*g*-MAH versus rotor speed, X_3X_5, and the interaction between EPDM-*g*-MAH and mixing temperature, X_2X_5, is presented in Figure 5(c,b), respectively. Maximum rotor speed (70 rpm) and minimum mixing temperature (70°C) versus maximum EPDM-*g*-MAH content (5 phr) should be applied to disperse the EPDM-*g*-MAH compatibilizer homogeneously in the blend so as to induce improved interaction between the rubber phases for maximum EB results. Hence, it can be justified that the processing parameters used in the NR/EPDM blends compounding must be balanced with the amount of EPDM-*g*-MAH compatibilizer as to gain maximum compatibilization effects for better or higher EB response.

Support Analysis Using RSM Optimization Tools, Swelling Test, DSC, and SEM Observation

Decision on Melt-Blending Operation for NR/EPDM Blends. In this study, the data retrieved from the tensile strength were further analyzed with RSM optimization tools. The objective of this step was to select the best combination of melt blending processing parameters, the appropriate amount of EPDM-*g*-MAH compatibilizer, and the NR/EPDM ratio that could yield a higher TS value. Tensile strength results were used to represent the compatibility and the quality of the produced NR/EPDM blends. A higher TS value might indicate the improved interaction between the rubber phases of NR and EPDM.[47] The predicted tensile strength at each experimental point is given in Table VI, along with the experimental data. The findings obtained are in accordance with Mohamad *et al.*[28]

Furthermore, this study established that the NR/EPDM blend with higher TS output response (coded as R5) could be prepared

Table VI. Comparison of Experimental and Predicted TS Values of NR/EPDM Blends

Experiments	Sample code	Experimental value (Y; MPa)	Predicted value (Y; MPa)
1	R1	5.31	5.30
2	R2	6.50	6.51
3	R3	5.50	5.51
4	R4	5.60	5.59
5	R5	7.28	7.27
6	R6	5.32	5.34
7	R7	5.89	5.90
8	R8	5.11	5.10
9	R9	5.01	5.01
10	R10	4.98	4.97
11	R11	5.13	5.13
12	R12	5.21	5.22
13	R13	5.51	5.51
14	R14	5.52	5.52
15	R15	4.24	4.24
16	R16	4.11	4.11
17	R17	6.21	6.36
18	R18	6.45	6.36
19	R19	6.42	6.36

by applying minimum EPDM content in the NR/EPDM ratio (70 : 30 of NR/EPDM), minimum mixing temperature (70°C), maximum rotor speed at 70 rpm, shorter mixing period (5 min), and lower amount of EPDM-*g*-MAH compatibilizer (1 phr). In this case, maximum rotor speed was required to improve the dispersion of dispersed phase (EPDM and EPDM-*g*-MAH) within the matrix (NR), and consequently, increased the tensile strength of NR/EPDM blend. High mechanical shearing induced by maximum rotor speed within the confined mixer space provided enough forces for better interaction between the rubber phases, and thus, improved the compatibility between them.

On the contrary, the NR/EPDM blend with the lowest TS output response (coded as R16) was yielded from the utilization of upper level for all independent variables; 50 : 50 NR/EPDM rubber components, maximum mixing temperature at 110°C, maximum rotor speed (70 rpm), maximum mixing period (9 min), and maximum content of EPDM-*g*-MAH compatibilizer (5 phr). Besides that explanation on the reduction of TS value for this parametric combination could be traced from relevant justification, as provided in the previous part of interaction studies between variables on response surface plots for Y_1, Y_2, Y_3, and Y_4. However, it is interesting to note that the addition of higher amount of EPDM-*g*-MAH compatibilizer would not necessarily give a maximum output for TS response. Thus, an appropriate EPDM-*g*-MAH compatibilizer content is essential to enhance the compatibilization effects in the produced blends with suitable combination of other processing parameters, which are directly involved in the preparation of NR/EPDM blends.

This can be done by applying the optimization menu in the Design Expert software by limiting the variables in range and targeting the TS response into the maximum goal. Approximately 10 final solutions were suggested by the software, complete with the predicted value of TS. A solution with higher desirability of about 0.960 and predicted TS value of 7.157 MPa was selected. Figure 6 depicts the ramp mode suggestion for the parametric combination of better TS output for NR/EPDM blends and the desirability chart for the response studied. The proposed set of parametric combination corresponded as $X_1 = 70$: 30 of NR/EPDM; $X_2 = 70$°C; $X_3 = 70$ rpm; $X_4 = 5$ min; and $X_5 =$ 1.34 phr of EPDM-*g*-MAH compatibilizer.

The proposed parametric combination by RSM was then validated by repeating the tensile testing accordingly. The suggested independent variables for maximum TS output response was repeatable with a very low deviation of only +2.303%, and the TS value was yielded at 7.322 MPa. As for the subsequent stage of support testing and analysis, the sample of NR/EPDM blend, which was prepared using the proposed parametric combination, was comparatively utilized and coded as RR.

Swelling Test and Cross-Link Density of NR/EPDM Blends. The swelling of rubber blends was frequently conducted to determine the crosslink density of the compound. It was found

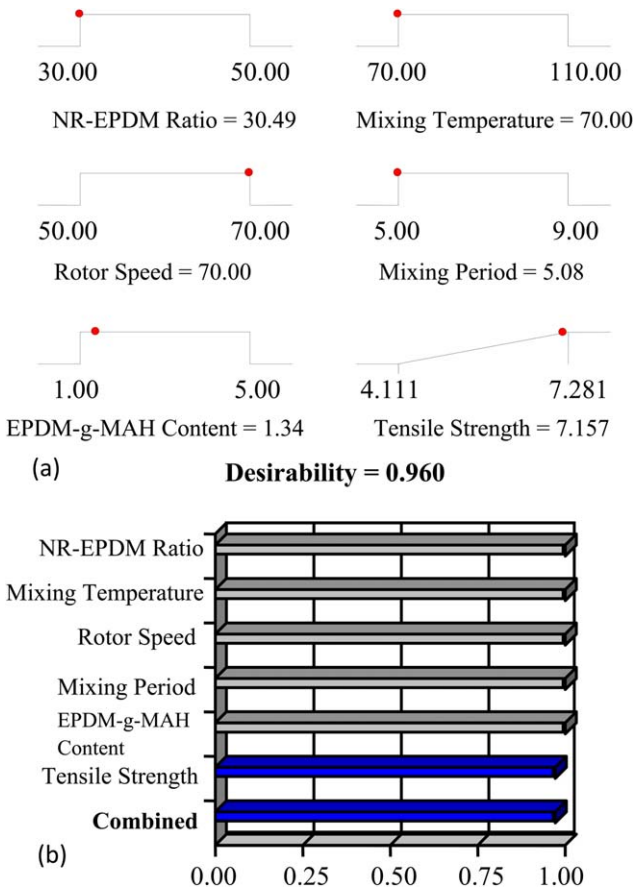

Figure 6. (a) Ramp mode suggestion of the best parametric combination for NR/EPDM blends with 0.960 desirability; (b) desirability chart for TS output response. [Color figure can be viewed in the online issue, which is available at wileyonlinelibrary.com.]

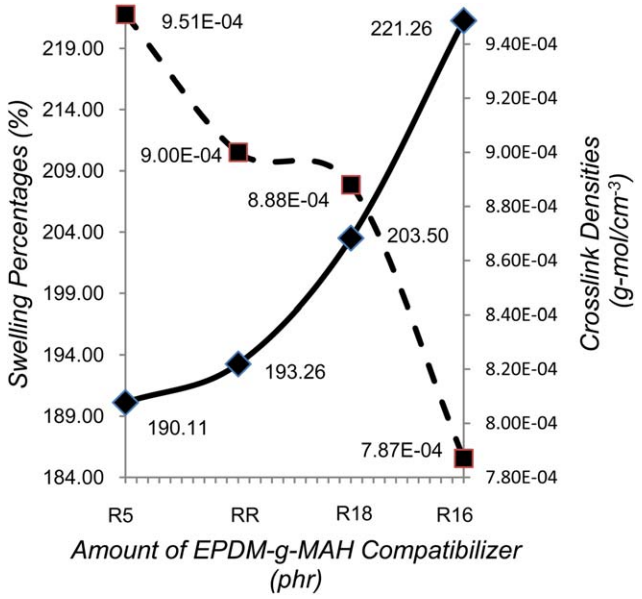

Figure 7. The swelling percentages and crosslink densities of the NR/EPDM blends with respect to the amount of EPDM-*g*-MAH compatibilizer addition. [Color figure can be viewed in the online issue, which is available at wileyonlinelibrary.com.]

that a higher crosslink density of a network chain lowered the percentage of swelling for vulcanized rubber in solvent.[46] In this study, a swelling test was performed to evaluate the effects of various loadings of the addition of EPDM-g-MAH compatibilizer to the crosslink density of the NR/EPDM rubber blends.

The crosslink density and the swelling percentages versus the amount of EPDM-*g*-MAH for R5, RR, R18, and R16 samples are shown in Figure 7. From the plot, it can be observed that the swelling percentage for R16 (5 phr) is higher than R5 (1 phr). This could be reasonably attributed to the efficacy of EPDM-*g*-MAH compatibilizer to give better compatibilization effects at lower additions. The presence of EPDM-*g*-MAH at a lower content improved the interaction between NR and EPDM rubber, which enhanced a three dimensional network in the blends. The cross linking network limited the absorption and the penetration of toluene towards the blends due to the limited open space between intermolecular rubber chains and gaps. This observation is in line with the increment in blend mechanical tensile properties due to the restriction to molecular motion of the blends chains by crosslink.[28]

The NR/EPDM blend, coded as R16, experienced a major increase in swelling percentage with exceedingly lower crosslink density as compared with other blends with the presence of a small amount of EPDM-*g*-MAH compatibilizer (R5, RR, and R18). The combination of maximum level of independent variables for processing parameters like higher mixing temperature, rotor speed, and mixing period for R16 blend seemed to deteriorate the formation of crosslink and to obstruct the possible interaction between the rubber phases. Maximum independent variables that were used to compound R16 might worsen the interaction between the rubber phases due to heat degradation and chain breakage via prolonged mixing time, high mixing temperature, and rotor speed. Furthermore, less ratio of NR in R16 blend (50 : 50) also caused the reduction of crosslink density within the blend, as it is known that NR is more polar, highly unsaturated, and more reactive than EPDM rubber.[19]

Thus, a higher EPDM content in blend formulation will result in lower possibility of crosslink formation and a higher percentage of swelling. In this case, it was once again proven that the amount of compatibilizer combined with suitable processing parameters, mainly contributed to the characteristics of the blends.

Differential Scanning Calorimetric Analysis of NR/EPDM Blends. DSC curves were analyzed to determine the glass transition temperature (T_g) of the selected NR/EPDM blends and their single rubber constituents. The samples were examined within the temperature range from −65 to 150°C. The T_g is an indirect representation of the heterogeneous nature of polymeric blend. A sharp single peak in endothermic curves indicates a highly miscible blend. Meanwhile, an intermediate peak with a value between those of the constituent components shows a partially miscible blend, and the separated peaks indicate an immiscible blend.[28]

The scan traces of the DSC thermogram for NR, EPDM, NR/EPDM blend without compatibilizers (R0), NR/EPDM blend with 1 phr of compatibilizer (R5), and NR/EPDM blend with 5 phr of compatibilizer (R16) are depicted in Figure 8. Both NR and EPDM rubber showed a single T_g peak at −58.0°C and −45.5°C, respectively. NR/EPDM blend without the compatibilizer (R0) was an immiscible blend with two distinct T_g values corresponding to the two neat constituents for the compositions of the blend. Meanwhile, R5 endotherms showed a significant single peak shift at about −49.0°C, as the temperature was

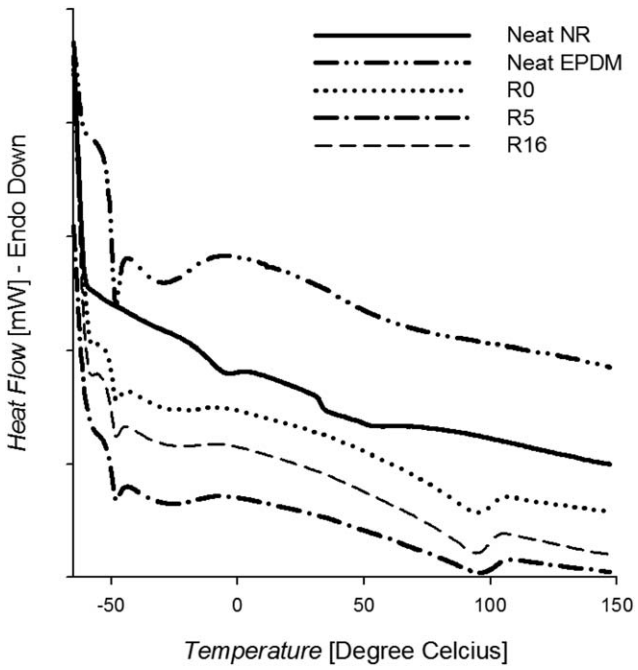

Figure 8. The DSC curves of EPDM, NR, and NR/EPDM with and without EPDM-*g*-MAH compatibilizer.

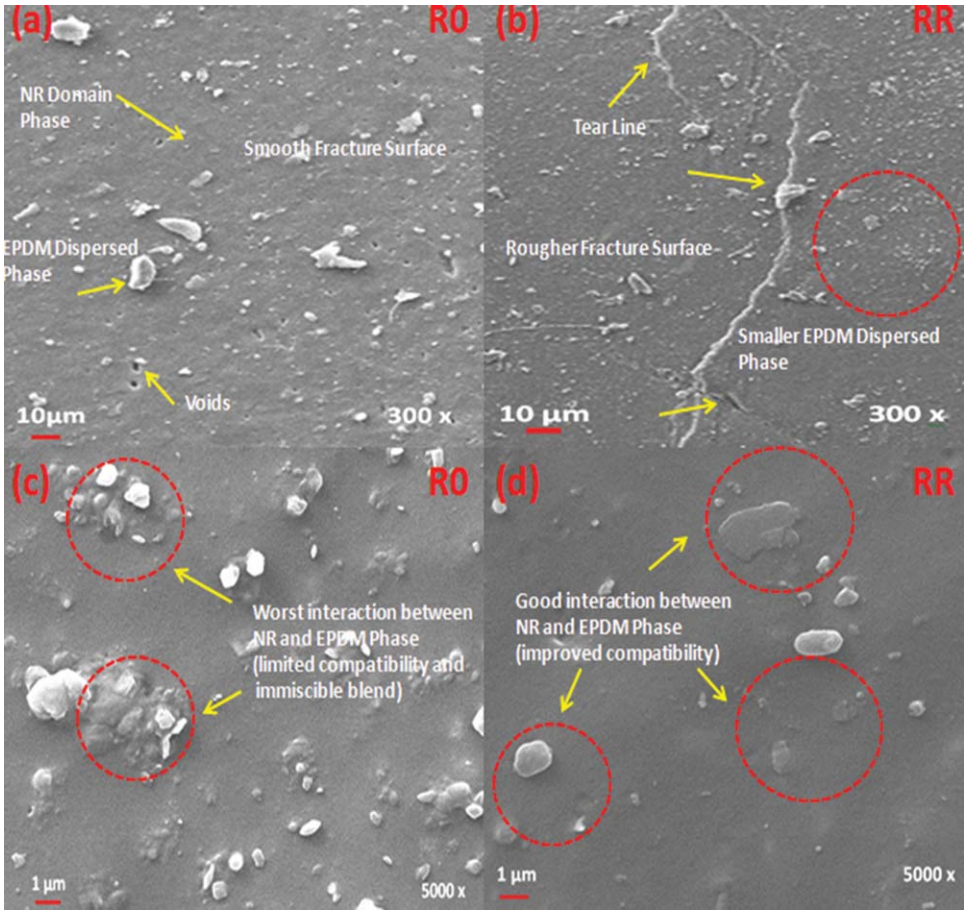

Figure 9. SEM micrographs showing tensile fracture surface morphologies of NR/EPDM blends at 70/30 blend ratio: (a) R0 at 300×, (b) RR at 300×, (c) R0 at 5000×, and (d) RR at 5000× of magnifications. [Color figure can be viewed in the online issue, which is available at wileyonlinelibrary.com.]

located between the T_g range for NR and EPDM rubber. Some interactions between NR and EPDM might have occurred at the boundaries of their phases as a third phase, indicating improved miscibility and compatibility between them.

The presence of EPDM-*g*-MAH at a lower amount, a minimum EPDM content in the blend ratio (70 : 30), and a combination of other processing parameters at their low level value, except for the rotor speed, were able to create a well-dispersed discontinuous phase that exhibited rheological properties almost similar to those obtained for compatible blend having one glass transition.[28] However, this did not happen to the NR/EPDM blend with the presence of a higher amount of compatibilizer (R16). Obviously, there were two intermediate T_g peaks present between the −60.0°C and −45.0°C temperature range that portrayed partial miscibility between these two rubbers.

This clearly shows that the utilization of all high-level values of processing parameters in NR/EPDM blends is actually ineffective in enhancing the miscibility and the compatibility between NR and EPDM rubber. A combination of maximum processing parameters like higher rotor speed, higher mixing temperature, and mixing period exposed the blend with major degradation effect and chains breakage due to excessive heat and shearing effects within prolonged mixing duration.

SEM Observations for Fracture Morphologies of NR/EPDM Blends. The SEM fracture morphological observation of NR/EPDM blends was performed to evaluate the transformation on tensile fracture surface with regards to the presence and the absence of EPDM-*g*-MAH compatibilizer. In this study, samples R0 and RR were selected and viewed at 300× and 5000× of magnification under SEM. Both NR/EPDM blends of 70 : 30 rubber ratio were compounded by using the best combination of processing parameters, as decided by the software with 1.34 phr of EPDM-*g*-MAH added for RR blend, while there was no addition of compatibilizer for R0 blend (control sample).

Figure 9 depicts the comparison of micrographs between R0 and RR at two different magnifications. At a lower magnification, it was observed that NR and EPDM rubber phases for R0 blend were clearly distinguished by the color contrast, whereby EPDM was brighter than NR, and obviously existed as a disperse phase within the NR dominant. In addition, several voids or holes were spotted at the micrograph, indicating a weak interaction between NR and EPDM rubber phases. Besides that, the fracture surface for R0 was smoother than RR, which clearly tells that less force was needed to break the R0 blend via tensile loading [Figure 9(a)]. Conversely, RR blend with the presence of EPDM-*g*-MAH showed the existence of many tearing lines [Figure 9(b)]. This represents the occurrence of shear yielding

between rubber interphase that caused rougher fracture surface due to better stress transfer and higher energy or forces applied to break the sample under the tensile loading. The presence of compatibilizer transformed the dispersed EPDM phase into finer droplets in size that were homogeneously distributed within the NR domain. The dispersed phase of EPDM altered the cracked paths and led to a higher resistance to crack propagation for RR, resulting in improved tensile strength,[28] compared than R0.

Furthermore, SEM micrographs at 5000× magnification for both samples provided a clearer comparison on the effects of the presence and absence of a compatibilizer. It was obviously seen that R0 blend experienced the worst interaction between NR and EPDM phase, as limited compatibility and immiscibility between both rubber phases caused un-wetted surface and agglomeration of minor phase of EPDM within the NR domain [Figure 9(c)]. This provided a reason for the existence of voids available at the R0 micrograph in Figure 9(a), due to the separation of EPDM rubber from NR during the tensile deformation.

However, this did not happen to the RR blend since improved compatibility and interaction between NR and EPDM rubber phases could be seen from good interaction, fully wetted, and less differences in phase contrast between both rubber phases. The addition of compatibilizer in RR seemed to develop a third phase between NR and EPDM rubber interphase, which consequently improved the properties of the produced blends, as established in this present study. This further proved that the added compatibilizer, more or less, successfully influenced the characteristics of the NR/EPDM blends, provided that the other melt-blending processing parameters by internal mixer were firstly optimized and determined through the systematic approach of RSM.

CONCLUSION

The relationships between the melt-blending processing parameters and the addition of EPDM-*g*-MAH compatibilizer to the mechanical tensile properties and cure characteristics of NR/EPDM blends were established using the related RSM analysis. It was found that the interactions between the independent variables in affecting the responses studied were consistent with the supported experimental findings. A higher R^2 value for each response is sufficient to represent the proposed regression model in predicting the optimum properties of NR/EPDM blends. The best combination of internal mixer processing parameters with an accurate amount of compatibilizer were decided in this work in ensuring the best possible performance of produced NR/EPDM blends with improved compatibility and miscibility between the rubber phases. The following statements can be drawn to summarize the overall significance of this study:

i. The presence of EPDM-*g*-MAH as a compatibilizer in NR/EPDM blends enhanced the cure characteristics. The cure time (tc_{90}) and maximum torque (M_H), increased as the EPDM-*g*-MAH content increased.
ii. A lower amount of compatibilizer was required to yield an optimum tensile strength (TS) value, with regards to optimum processing parameters, except for the NR/EPDM ratio of 50 : 50, while a higher amount of EPDM-*g*-MAH should be added to the blend to maximize the percentage of elongation at break (EB) by accurately manipulating the maximum and the minimum of other processing variables.
iii. The best combinations of processing parameters based on TS response (Y_1) for NR/EPDM blends prepared by melt-blending with the compatibilizer were suggested by the software as 70 : 30 of NR/EPDM (X_1), 70°C of mixing temperature (X_2), 70 rpm of rotor speed (X_3), 5 min of mixing period (X_4), and 1.34 phr of EPDM-*g*-MAH compatibilizer (X_5). A higher reproducibility of the proposed parameters was fortified by a higher R^2 value of 99.60%, a small deviation at +2.303%, and a higher desirability of 0.960.
iv. Supporting experimental analysis through DSC analysis, swelling and crosslink density measurements, and SEM observation for fracture surface morphologies showed good correlations in accordance to the RSM results and the role of compatibilizer was highlighted in affecting and improving the properties of NR/EPDM blends. Compatibilized NR/EPDM blend with 1 phr of EPDM-*g*-MAH revealed the formation of a single Tg peak in the curve, which corresponded to a miscible blend and improved the compatibility between NR and EPDM rubber phases. In addition, swelling and cross linking density measurements successfully proved that the lowest addition of compatibilizer (1 phr) increased the formation of crosslink to 9.51E-04 g-mol/cm^{-3}, and decreased the percentage of swelling to the lowest at 190.11%, compared with a blend with high maximum amount of compatibilizer. Moreover, the transformation in fracture surface morphologies for compatibilized NR/EPDM blend indicated a better and stronger adhesion between NR and EPDM rubber, which was promoted by the presence of a compatibilizer at 1.34 phr for the RR blend.

ACKNOWLEDGMENTS

The authors thank the Malaysian Ministry of Education for awarding the SLAB/SLAI scholarship, and the research funding provided by the Fundamental Research Grant Scheme FRGS/2012/FKP/TK04/02/1/F00132 awarded to Universiti Teknikal Malaysia Melaka (UTeM). Special appreciation goes to the Carbon Research Technology (CRT) research group FKP in UTeM, and Polymer Research Group, FST in Universiti Kebangsaan Malaysia (UKM) for their continuous support, motivation, and collaboration. The authors also thank UKM, UTeM, and Malaysian Nuclear Agency (MNA) for their expertise, research facilities, and continuous technical support towards the accomplishment of this research.

REFERENCES

1. Mathew, G.; Singh, R. P.; Nair, N. R.; Thomas, S. *J. Mater. Sci.* **2003**, *38*, 2469.
2. Habeeb Rahiman, K.; Unnikrishnan, G.; Sujith, A.; Radhakrishnan, C. K. *Mater. Lett.* **2005**, *59*, 633.
3. Varghese, H.; Bhagawan, S. S.; Someswara Rao, S.; Thomas, S. *Eur. Polym. J.* **1995**, *31*, 957.
4. Hussein, I. A.; Chaudhry, R. A.; Abu Sharkh, B. F. *Polym. Eng. Sci.* **2004**, *44*, 2346.

5. Arayapranee, W.; Rempel, G. L. *J. Appl. Polym. Sci.* **2008**, *109*, 932.
6. Botros, S. H.; El Sayed, A. M. *J. Appl. Polym. Sci.* **2001**, *82*, 3052.
7. Nabil, H.; Ismail, H.; Azura, A. R. *Polym. Test.* **2013**, *32*, 385.
8. Manshaie, R.; Nouri Khorasani, S.; Jahanbani Veshare, S.; Rezaei Abadchi, M. *Radiat. Phys. Chem.* **2011**, *80*, 100.
9. Zhang, H.; Datta, R. N.; Talma, A. G.; Noordermeer, J. W. M. *Eur. Polym. J.* **2010**, *46*, 754.
10. Suk Lee, Y.; Lee, W.-K.; Cho, S.-G.; Kim, I.; Ha, C.-S. *J. Anal. Appl. Pyrolysis* **2007**, *78*, 85.
11. Jovanović, V.; Samaržija-Jovanović, S.; Budinski-Simendić, J.; Marković, G.; Marinović-Cincović, M. *Compos. B* **2013**, *45*, 333.
12. Abou Zeid, M. M. *Eur. Polym. J.* **2007**, *43*, 4415.
13. Aoshuang, Y.; Zhengtao, G.; Li, L.; Ying, Z.; Peng, Z. *Radiat. Phys. Chem.* **2002**, *63*, 497.
14. Alipour, A.; Naderi, G.; Bakhshandeh, G. R.; Vali, H.; Shokoohi, S. *Int. Polym. Process* **2011**, *XXVI*, 48.
15. Costa, V. G.; Rees Nunes, R. C. *Eur. Polym. J.* **1994**, *30*, 1025.
16. Arayapranee, W.; Rempel, G. L. *Int. J. Mater. Struct. Reliab.* **2007**, *5*, 1.
17. Motaung, T. E.; Luyt, A. S.; Thomas, S. *Polym. Compos.* **2011**, *32*, 1289.
18. Nabil, H.; Ismail, H.; Azura, A. R. *Mater. Des.* **2013**, *50*, 27.
19. Sae-oui, P.; Sirisinha, C.; Thepsuwan, U.; Thapthong, P. *Polym. Test.* **2007**, *26*, 1062.
20. Sae-oui, P.; Sirisinha, C.; Thepsuwan, U.; Hatthapanit, K. *Eur. Polym. J.* **2007**, *43*, 185.
21. Shehata, A. B.; Afifi, H.; Darwish, N. A.; Mounir, A. *Polym. Plast. Technol. Eng.* **2006**, *45*, 165.
22. Zaharescu, T.; Meltzer, V.; Vilcu, R. *Polym. Degrad. Stab.* **2000**, *70*, 341.
23. Grigoryeva, O. P.; Karger-Kocsis, J. *Eur. Polym. J.* **2000**, *36*, 1419.
24. Pasbakhsh, P.; Ismail, H.; Ahmad Fauzi, M. N.; Abu Bakar, A. *Polym. Test.* **2009**, *28*, 548.
25. Sirqueira, A. S.; Soares, B. G. *J. Macromol. Sci. Phys.* **2007**, *46*, 639.
26. Alipour, A.; Naderi, G.; Ghoreishy, M. H. *J. Appl. Polym. Sci.* **2013**, *127*, 1275.
27. Nabil, H.; Ismail, H.; Azura, A. R. *Polym. Test.* **2013**, *32*, 631.
28. Mohamad, N.; Yaakub, J.; Abd Razak, J.; Yaakob, M. Y.; Shueb, M. I.; Muchtar, A. *J. Appl. Polym. Sci.* **2014**, *40713*, 1.
29. Sirqueira, A. S.; Soares, B. G. *J. Appl. Polym. Sci.* **2002**, *83*, 2892.
30. Nakason, C.; Kaesaman, A.; Samoh, Z.; Homsin, S.; Kiatkamjornwong, S. *Polym. Test.* **2002**, *21*, 449.
31. Koning, C.; Van Duin, M.; Pagnoulle, C.; Jerome, R. *Prog. Polym. Sci.* **1998**, *23*, 707.
32. Phua, Y. J.; Chow, W. S.; Mohd Ishak, Z. A. *eXPRESS Polym. Lett.* **2013**, *7*, 340.
33. Matarredona, O.; Rhoads, H.; Li, Z.; Harwell, J. H.; Balzano, L.; Resasco, D. E. *J. Phys. Chem. B* **2003**, *107*, 13357.
34. El-Sabbagh, S. H. *Polym. Test.* **2003**, *22*, 93.
35. Mangaraj, D. *Rubber Chem. Technol.* **2002**, *75*, 365.
36. Tavakoli, M.; Katbab, A. A.; Nazockdast, H. *J. Macromol. Sci. Phys.* **2011**, *50*, 1270.
37. Abd Razak, J.; Mohamad, N.; Ab Maulod, H. E. *J. Elastomers Plast.* **2012**, *45*, 239.
38. Nawawi, M. A.; Sim, L. H.; Chan, C. H. *Int. J. Chem. Eng. Appl.* **2012**, *3*, 410.
39. Gunasekaran, S.; Natarajan, R. K.; Kala, A. *Spectrochim. Acta Part A* **2007**, *68*, 323.
40. Kumar, A.; Dipak, G.; Basu, K. *J. Appl. Polym. Sci.* **2002**, *84*, 1001.
41. Ghoneim, A. M.; Ismail, M. N. *Polym. Plast. Technol. Eng.* **1999**, *38*, 979.
42. Mohamad, N.; Muchtar, A.; Ghazali, M. J.; Hj Mohd, D.; Azhari, C. H. *J. Appl. Polym. Sci.* **2010**, *115*, 183.
43. Myers, R. H.; Montgomery, D. C.; Anderson-Cook, C. M. Response Surface Methodology: Process and Product Optimization using Designed Experiments, 3rd ed.; Wiley Series in Probability and Statistics; Wiley: New York, **2009**; p 798.
44. Ahmed, K.; Sirajuddin Nizami, S.; Raza, N. Z.; Shirin, K. *Adv. Mater. Phys. Chem.* **2012**, *2*, 90.
45. Basfar, A. A.; Abdel-Aziz, M. M.; Mofti, S. *Radiat. Phys. Chem.* **2002**, *63*, 81.
46. Konar, B. B.; Roy, S. K.; Pariya, T. K. *J. Macromol. Sci. Pure Appl. Chem.* **2010**, *47*, 416.
47. Abd Razak, J.; Ahmad, S. H.; Ratnam, C. T.; Mahamood, M. A.; Yaakub, J.; Mohamad, N. *AIP Conf. Proc.* **2014**, *1614*, 82.